ROBERT BOSCH CENTRE FOR CYBER-PHYSICAL SYSTEMS
3rd Floor, Entrepreneurship Building, Indian Institute of Science

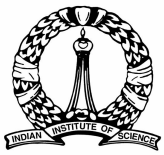

Technical Report No: RBCCPS/TR/0002

Publication Date: February 2016

Title: Continuous Ambulatory Electrocardiography

Authors: Sagar Venkatesh Gubbi, Hiteshwar Rao, and Bharadwaj Amrutur

Continuous Ambulatory Electrocardiography

Sagar Venkatesh Gubbi, Hiteshwar Rao, and Bharadwaj Amrutur, *Senior Member, IEEE*

Abstract

Continuous ambulatory recording of the electrocardiogram could help in early detection of cardiovascular diseases, which could lower healthcare costs and improve prognosis. For such continuous recordings, sensors that are discreet and have few electrodes are needed. Two electrode ECG systems exhibit worse power line interference than three electrode systems, but are desirable because they have one less electrode. A circuit model that captures power-line interference is reviewed, which is then used to analyze the performance characteristics of different interface circuits. For two electrode systems, an adaptive filter is found to be effective in digitally removing any remnant power line interference. Finally, our analysis shows that the low-impedance electrode in a 3-electrode system may be sized differently than the high impedance electrodes while keeping the power-line interference sufficiently small. This observation leads to a pseudo 2-electrode electrocardiograph which is in fact a 3-electrode system with an inconspicuous third electrode.

I. Introduction

Societies are growing older because of increasing life expectancy, and the aging of societies is accompanied by rising healthcare costs [1]–[5]. A significant fraction of the healthcare expenditure is for treating cardiovascular diseases [4]. Continuous ambulatory electrocardiography can be used to detect heart diseases early on, which leads to better prognosis while simultaneously reducing health care costs [6]. Such continuous monitoring using wearable sensors has recently been made practical by the explosive growth of smartphones, which can serve as a convenient gateway device that talks to low-power wearable sensors and uploads the sensed data to a cloud database where the data can be analyzed [7].

Continuous ambulatory electrocardiography differs from traditional in-hospital electrocardiographs (Fig. 1) in several ways. The sensors have to be discreet, comfortable to wear, and consume little power so that the battery size may be reduced [8]–[13]. To keep the sensor discreet, it is desirable to have as few electrodes as possible. Fortunately, even a one lead electrocardiograph can be used to detect many of the common cardiovascular diseases [14].

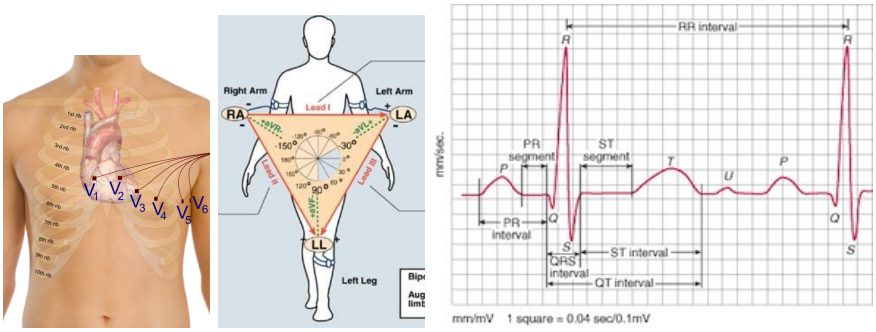

(a) Electrodes near the heart (b) Electrodes on the limbs (c) A sample electrocardiogram

Fig. 1. Sample electrode locations and a sample electrocardiogram.

A major issue in acquiring ECG signals is the presence of power-line interference. Because the human body is a good conductor of electricity compared to air, a small displacement current due to nearby power lines (on the order of 100 nA) flows through the body to the earth [15]. This manifests itself as a common mode voltage as seen by the electrocardiograph and can be substantially higher than the ECG signal itself. We shall model this phenomenon and analyze how well different circuit topologies suppress this interference (Sections 2 and 3). Typically, ECG systems have at least 3 electrodes: two sensing electrodes, and one driven electrode, so as to minimize the power line interference. Using only two electrodes results in high interference, which would require elaborate circuitry to suppress [16]. We propose sizing the sensing and driven electrodes differently so that the electrocardiograph is kept discreet while still keeping the interference at bay. The American Heart Association recommends an amplitude error limit of 10 μV or 2% (whichever is higher) [17]. Typically, ECG signals have an amplitude of about 1 mV. So, power-line interference has to be kept below 20 μV.

Another issue in continuous ambulatory electrocardiography lies in the electrodes. In clinical settings, adhesive “wet” electrodes are most commonly used. Good electrical contact between the skin and the electrode is assured by either abrading the skin

This report was written in May 2014. S.V.Gubbi is with the Dept. Of ECE, H.Rao is with the Robert Bosch Center for Cyber-Physical Systems, and B.Amrutur is with ECE / Robert Bosch Center for Cyber-Physical Systems. e-mail: sagar.writeme@gmail.com, rao.hiteshwar@gmail.com, and amrutur@ece.iisc.ernet.in.
This work was funded by the Robert Bosch Centre for Cyber-Physical Systems, Indian Institute Of Science, Bangalore, India.

and/or using a conductive gel. However, both of these methods cause significant inconvenience and are completely unsuitable for long-term ambulatory monitoring. To overcome this problem, dry-contact electrodes that require no skin preparation or conductive gels have been proposed [8]–[11], [18]–[25]. But dry-contact electrodes have significantly larger impedance than wet-contact electrodes. This can be surmounted by using very high impedance amplifiers (Section 4). However, the lack of adhesion in dry-contact electrodes leads to increased motion artifacts [26], and this is an open problem.

The rest of this report is organized as follows. In Section 2, a circuit model that captures the effect of power-line interference is described. Subsequently, several interface circuit topologies are analyzed using this model (Section 3). Then, a very high impedance amplifier suited for dry-contact ECG front-ends is discussed (Section 4). Experimental results are presented in Section 5. Afterwords, a couple of pratical tips for building electrocardiographs are given (Section 6). Finally, some open issues are discussed in Section 7, and Section 8 concludes this report.

II. Circuit Model

Electrical power lines carrying high voltage at 50 Hz are ubiquitous. Because the human body is a good conductor of electricity compared to air, a small displacement current flows from the power lines through the human body to the ground. Along with the source of the ECG signal, this may be modeled by the circuit in Fig. 2. Values for the parasitic capacitances are from [15].

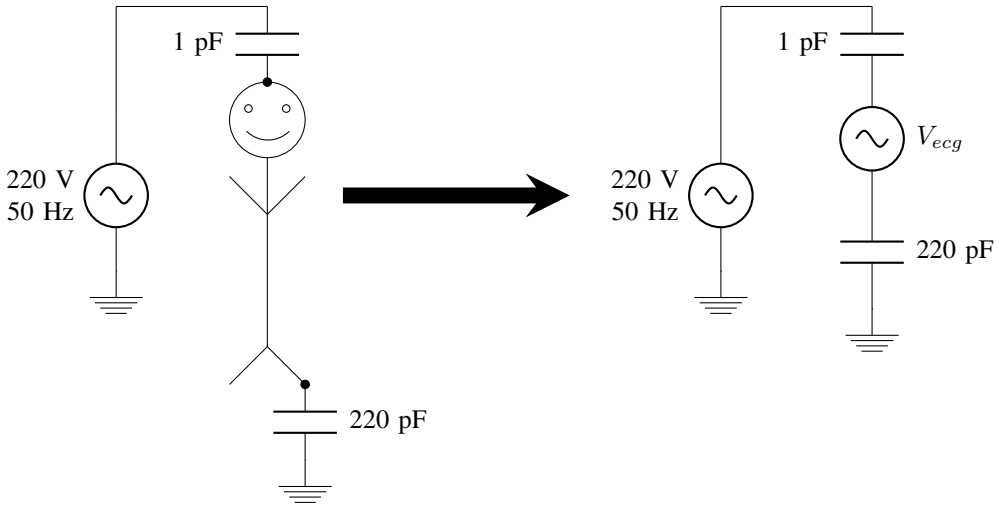

Fig. 2. Electrical model of the human body.

III. Performance of interface circuit configurations

The performance of different interface circuit configurations is analyzed using the electrical model developed in the previous section. Z_e is the electrode-skin impedance (if there are two sensing electrodes, the impedances are Z_{e1} and Z_{e2}), Z_i is the input impedance of a unity gain buffer, Z_g is the electrode-skin impedance of the low-impedance electrode, and Z_s is the isolation impedance between the circuit common and the earth ground. All node voltages with a single subscript are with respect to earth ground and *not* circuit common (Example: V_g). Z_i of hi-z buffers is in the order of 1 GΩ. For copper dry-contact electrodes of 1 cm^2 size, Z_e is typically around 1 MΩ [26]. In battery operated circuits that are isolated from the earth ground, Z_s is around 3 pF (1 GΩ at 50 Hz) [15].

A. Two-electrode Single Ended Interface Circuit

In this configuration (Fig. 3), one of the electrodes is connected to a high impedance unity gain amplifier (described in Section 4). The second electrode is a low impedance electrode that is connected to the circuit common (V_g).

Since the isolation impedance between the ECG interface circuit and the earth ground is substantially larger than the human body to earth ground impedance,

$$V_c \approx \frac{\frac{1}{220p}}{\frac{1}{1p}+\frac{1}{220p}} \times 220V, 50Hz \approx 1V, 50Hz \tag{1}$$

Some of the displacement current due to the 220 V power line flows from the body to the earth ground via the interface circuit.

$$\frac{V_c - V_g}{Z_g} = \frac{V_g}{Z_s} \tag{2}$$

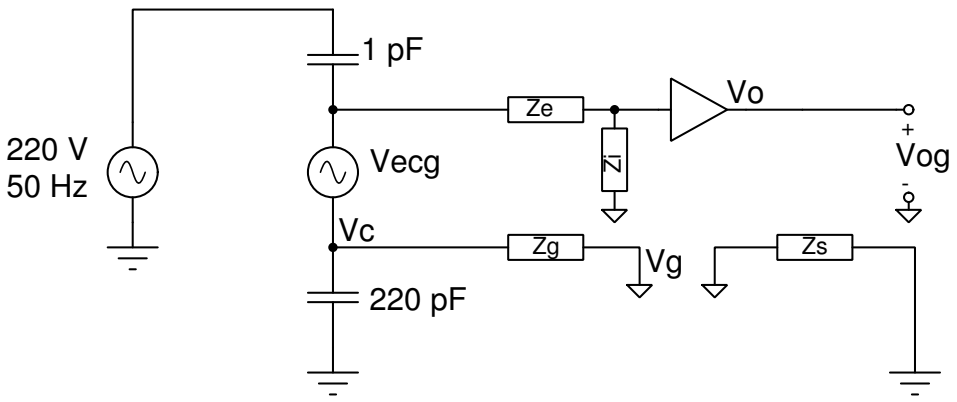

Fig. 3. Two-electrode single ended interface circuit

Thus,

$$V_g = \frac{Z_s}{Z_s + Z_g} V_c \tag{3}$$

Equation (3) shows that as isolation impedance between the circuit common and the earth ground increases, the circuit common comes closer to the potential of the body and thus less of the 50 Hz common mode power line interference is seen.

Finally,

$$V_{og} = V_o - V_g = \frac{Z_i}{Z_e + Z_i}(V_c + V_{ecg} - V_g) = \frac{Z_i}{Z_e + Z_i}\left(\frac{Z_g}{Z_s + Z_g} V_c + V_{ecg}\right) \tag{4}$$

Simplifying,

$$V_{og} = \left(\frac{Z_i}{Z_e + Z_i} \cdot \frac{Z_g}{Z_s + Z_g}\right) V_c + \left(\frac{Z_i}{Z_e + Z_i}\right) V_{ecg} \tag{5}$$

Even if the two electrode impedances are matched (i.e.. $Z_g = Z_e$), the output seen by the circuit contains substantial power-line interference. Thus, this circuit is not recommended. A sample implementation of the 2-electrode single ended interface circuit may be found in [27].

B. Two-electrode Differential Interface Circuit

In this configuration (Fig. 4), both the electrodes are connected to high impedance unity gain amplifiers. The circuit common is left floating and is connected to earth ground only via a large isolation impedance (Z_s).

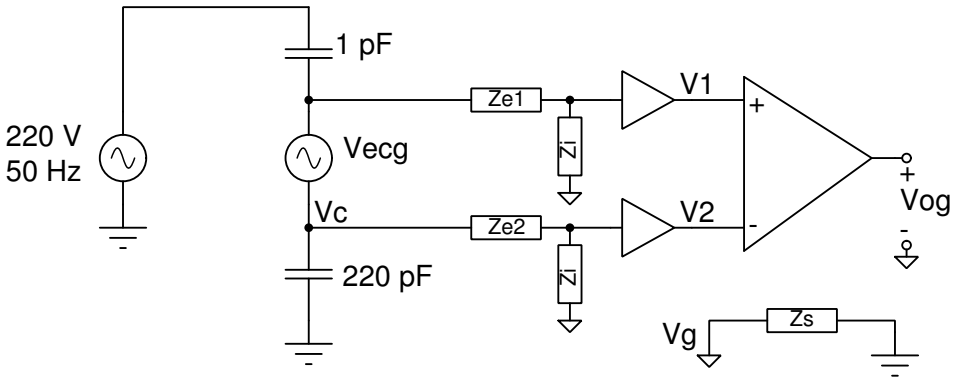

Fig. 4. Two-electrode differential interface circuit

The isolation impedance drags the circuit common weakly towards earth ground.

$$V_g = 0 \tag{6}$$

After the unity gain buffers,

$$V_2 = \frac{Z_i}{Z_{e2} + Z_i} V_c \tag{7}$$

$$V_1 = \frac{Z_i}{Z_{e1} + Z_i}(V_c + V_{ecg}) \tag{8}$$

Thus, for small electrode imbalances ($Z_{e1} \approx Z_{e2}$),

$$V_{og} = V_1 - V_2 = \frac{\frac{\Delta Z_e}{Z_i}}{\left(1 + \frac{Z_e}{Z_i}\right)^2} V_c + \frac{Z_i}{Z_i + Z_{e1}} V_{ecg} \tag{9}$$

where $\Delta Z_e = Z_{e2} - Z_{e1}$ and $Z_e = \frac{Z_{e1}+Z_{e2}}{2}$. Although in this configuration, when the electrode impedances are matched the interference vanishes, it is inadvisable to use this because (a) The circuit common is floating, and (b) High common mode impedance is unforgiving to static voltages that develop on the body, and this can cause the amplifiers to saturate [15]. These problems can be surmounted by having a topology with low common mode input impedance and high differential mode impedance [28]–[30]. However, this is not recommended because differential input impedance is limited by component tolerances. It turns out that both high common mode impedance and low common mode impedance result in low power-line interference [31], but low common mode impedance is more suitable since it is resistant to static charges on the body. The right leg drive based three-electrode interface discussed in a subsequent section has simpler circuitry and offers better performance.

C. Three-electrode Interface circuit with passive ground

In this configuration (Fig. 14), the two sensing electrodes are connected to high impedance unity gain amplifiers. The third low-impedance electrode is connected to the circuit common.

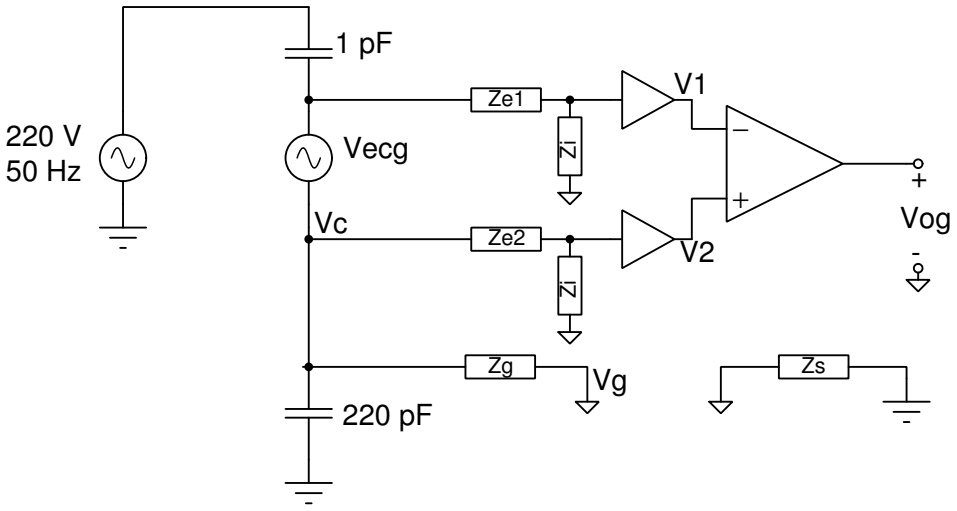

Fig. 5. Three-electrode interface circuit with passive dry ground

Similar to subsection A,

$$V_g = \frac{Z_s}{Z_s + Z_g} V_c \tag{10}$$

And,

$$V_1 = Vg + \frac{Z_i}{Z_i + Z_{e1}} (V_c + V_{ecg} - V_g) \tag{11}$$

$$V_2 = Vg + \frac{Z_i}{Z_i + Z_{e2}} (V_c - V_g) \tag{12}$$

Thus,

$$V_{og} = \left(\frac{Z_i}{Z_i + Z_{e1}} - \frac{Z_i}{Z_i + Z_{e2}} \right) \frac{Z_g}{Z_s + Z_g} V_c + \frac{Z_i}{Z_i + Z_{e1}} V_{ecg} \tag{13}$$

For small electrode mismatches ($Z_{e1} \approx Z_{e2}$),

$$V_{og} = \left(\frac{\frac{\Delta Z_e}{Z_i}}{\left(1 + \frac{Z_e}{Z_i}\right)^2} \cdot \frac{Z_g}{Z_s + Z_g} \right) V_c + \frac{Z_i}{Z_i + Z_{e1}} V_{ecg} \tag{14}$$

where $\Delta Z_e = Z_{e2} - Z_{e1}$ and $Z_e = \frac{Z_{e1}+Z_{e2}}{2}$. When the two electrodes are matched, the power-line interference vanishes. Furthermore, when the isolation impedance (Z_s) is large as in the case of battery powered systems, the low-impedance

connection to the body (Z_g) suppresses the interference when there is an electrode mismatch. While this configuration can be used, the driven right leg circuit described in the next subsection is even more effective at suppressing power line interference in the presence of electrode mismatches, and thus it should be preferred.

D. Three-electrode Interface circuit with driven right leg

In this configuration (Fig. 6), the two sensing electrodes are connected to high impedance unity gain amplifiers. The third low-impedance electrode is driven an amplified and inverted version of the common mode signal.

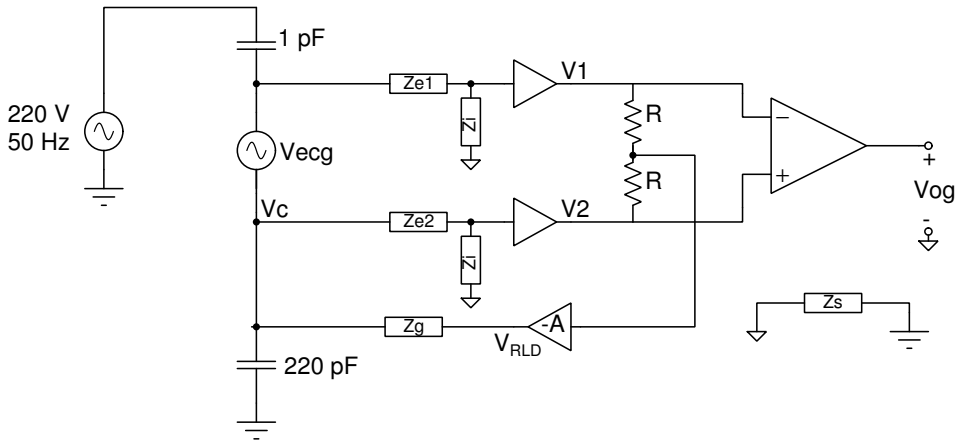

Fig. 6. Three-electrode interface circuit with driven ground

To simplify calculations, we shall initially assume that $Z_i = \infty$. Then,

$$V_2 = V_c \tag{15}$$

and

$$V_1 = V_c + V_{ecg} \tag{16}$$

The right leg drive amplifier amplifiers the common mode voltage to give

$$V_{RLD} = -A\left(\frac{V_1 + V_2}{2}\right) + V_g \tag{17}$$

$$V_{RLD} = -A\left(V_c - V_g + \frac{V_{ecg}}{2}\right) + V_g \tag{18}$$

Now, we can calculate the circuit common potential V_g.

$$\frac{V_c - V_{RLD}}{Z_g} = \frac{V_g}{Z_s} \tag{19}$$

Assuming that $A >> 1$,

$$\frac{V_c}{Z'_g} + \frac{V_{ecg}}{2Z'_g} = \frac{V_g}{Z_s} + \frac{V_g}{Z'_g} \tag{20}$$

where $Z'_g = \frac{Z_g}{A+1}$. Thus,

$$V_g = \frac{Z_s}{Z_s + Z'_g}V_c + \frac{Z_s}{Z_s + Z'_g}\frac{V_{ecg}}{2} \tag{21}$$

Let us now return to the case when $Z_i < \infty$ and calculate the output voltage.

$$V_{1g} = V_1 - V_g = (V_c + V_{ecg} - V_g)\frac{Z_i}{Z_i + Z_{e1}} \approx \left(\frac{Z'_g}{Z_s}V_c + \frac{V_{ecg}}{2}\right)\frac{Z_i}{Z_i + Z_{e1}} \tag{22}$$

$$V_{2g} = V_1 - V_g = (V_c - V_g)\frac{Z_i}{Z_i + Z_{e1}} \approx \left(\frac{Z'_g}{Z_s}V_c - \frac{V_{ecg}}{2}\right)\frac{Z_i}{Z_i + Z_{e2}} \tag{23}$$

If the electrode imbalance is small,

$$V_{og} = V_{1g} - V_{2g} = \left(\frac{Z'_g}{Z_s}\frac{\frac{\Delta Z_e}{Z_i}}{\left(1+\frac{Z_e}{Z_i}\right)^2}\right)V_c + \left(\frac{Z_i}{Z_i + Z_e}\right)V_{ecg} \tag{24}$$

where $\Delta Z_e = Z_{e2} - Z_{e1}$ and $Z_e = \frac{Z_{e1}+Z_{e2}}{2}$. This is similar to Eq. (14) with Z_g replaced by Z'_g. Thus, with right leg drive, the electrode-skin impedance of the low-impedance electrode effectively gets divided by the right leg drive gain (A). A more detailed discussion of common mode interference and the right leg drive circuit may be found in [32], [33] and [34].

TABLE I
NOISE ESTIMATION PERFORMANCE

Circuit configuration	V_{og}	Typical values
2-electrode, single ended	$V_{og} = \left(\frac{Z_i}{Z_e+Z_i}\cdot\frac{Z_g}{Z_s+Z_g}\right)V_c + \left(\frac{Z_i}{Z_e+Z_i}\right)V_{ecg}$	$V_{og} = 10\ mV_{50Hz} + 1\ mV_{ecg}$
2-electrode, differential	$V_{og} = \left(\frac{\frac{\Delta Z_e}{Z_i}}{\left(1+\frac{Z_e}{Z_i}\right)^2}\right)V_c + \left(\frac{Z_i}{Z_i+Z_{e1}}\right)V_{ecg}$	$V_{og} = 5\ mV_{50Hz} + 1\ mV_{ecg}$
3-electrode, passive ground	$V_{og} = \left(\frac{\frac{\Delta Z_e}{Z_i}}{\left(1+\frac{Z_e}{Z_i}\right)^2}\cdot\frac{Z_g}{Z_s+Z_g}\right)V_c + \left(\frac{Z_i}{Z_i+Z_{e1}}\right)V_{ecg}$	$V_{og} = 50\ \mu V_{50Hz} + 1\ mV_{ecg}$
3-electrode, driven-right-leg	$V_{og} = \left(\frac{\frac{\Delta Z_e}{Z_i}}{\left(1+\frac{Z_e}{Z_i}\right)^2}\cdot\frac{Z'_g}{Z_s+Z'_g}\right)V_c + \left(\frac{Z_i}{Z_i+Z_e}\right)V_{ecg}$	$V_{og} = 0.5\ \mu V_{50Hz} + 1\ mV_{ecg}$

Table I compares the performance of the four interface circuit configurations discussed. The general trend is that power-line interference reduces as the electrode imbalance decreases and the influence of electrode imbalance becomes smaller as the input impedance of the front-end amplifier increases.

Let us consider some typical numerical values for battery powered copper dry-contact electrodes of size 1 cm^2. Suppose $Z_i = 100\ M\Omega$, $Z_e = Z_g = 10\ M\Omega$, $\Delta Z_e = 500\ k\Omega$, $Z_s = 1\ G\Omega$, $V_c \approx 1V, 50Hz$, and for the right leg drive $A = 100$. The third column in Table I gives a feel for the performance of different interface circuit configurations using these parameters. The first term in the third column represents the amplitude of the power-line interference and the second term represents the amplitude of the ECG signal (assumed to be 1 mV). The right leg drive configuration results in the least power-line interference.

Several methods have been proposed to remove the remnant power-line interference due to electrode imbalance. Sophisticated phase sensitive detection has been used in [35] to tilt the gain in the differential amplifier and favor one of the electrodes so as to neutralize the electrode imbalance. A Phase Locked Loop (PLL) and a lock-in amplifier (LIA) have been used in [16] to lock on to the interference signal and cancel it. An adaptive filter in the digital domain can also be used to cancel power-line interference [36]–[39]. Among these techniques, the adaptive filter in [39] is preferable because it is robust and needs no additional hardware.

Finally, ultra-low power discrete and integrated implementations of variants of these circuits are described in [13] and [12] respectively.

IV. INPUT IMPEDANCE

The input impedance of the front-end amplifier forms a potential divider with the electrode impedance. Furthermore, as seen in the previous section, a smaller input impedance exacerbates the effect of electrode imbalance resulting in larger power-line interference. Thus, it is desirable to have large input impedance in the front-end amplifiers. This is achieved in the so-called "active electrodes" by placing the amplifier right on top of the electrode, thereby reducing the loss of input impedance in the cable that attaches the electrode to the circuitry [40]. Degen et al. go one step further and amplify the ECG signal on the electrode itself at the cost of larger interference due to gain mismatch [41].

The use of bootstrapped amplifiers has been proposed in [15], [42] to achieve large input impedance in the front-end amplifier. However, bootstrapping worsens noise performance. In [40] and more recently in [22], [26], rail-to-rail input/output (RRIO) opamps have been used with the positive terminal left floating (Fig. 7). This is based on the idea that a small leakage current through the input protection diodes on the hi-z positive terminal will bias the op-amp. It is possible, even likely, that the bias point will be close to one of the rails because of mismatch in the input protection diodes and other parasitics. However, the ECG signal, with an amplitude of only a few mV at most, will have no trouble passing through the RRIO unity gain amplifier. This signal is subsequently high-pass filtered so as to not overwhelm the subsequent stages with a signal close to the rails.

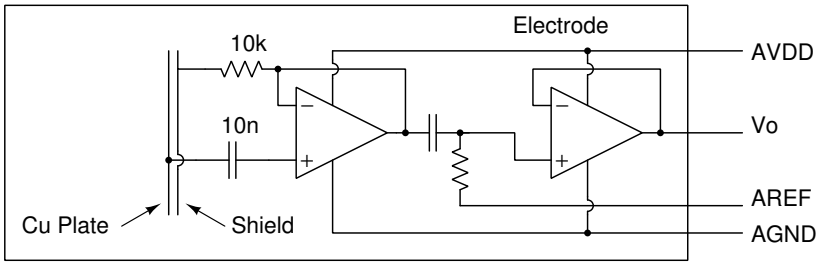

Fig. 7. Schematic of the electrode. The sensing copper plate is the backside of the PCB. The components are assembled on the front side. The copper plate will be in contact with the skin, and the driven shield in the inner plane of the PCB serves to reduce input capacitance.

V. Experimental Results

Figure 8 shows the schematic of the prototype electrocardiograph[1]. A 12-bit ADC was used with a sample rate of 400 Hz. Although Fig. 8 depicts the inner plane of the PCB being used as a shield, our implementation was on a 2-layer PCB with no such shield.

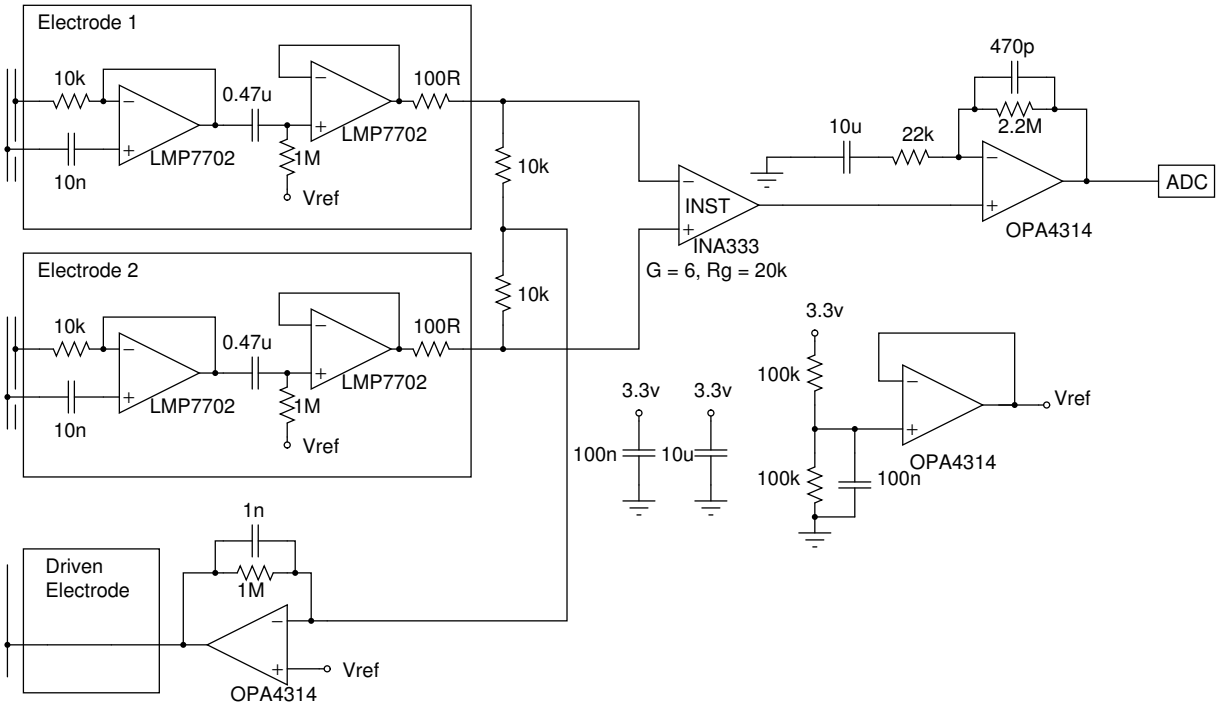

Fig. 8. Schematic of the prototype electrocardiograph.

As discussed previously, in the driven right leg configuration, the electrode impedance of the low-impedance driven electrode is effectively divided by the gain of the feedback amplifier. Thus, the low-impedance electrode may be sized considerably smaller than the high impedance sensing electrodes. We christen this "pseudo 2-electrode" ECG, wherein the outer ring of one of the electrodes is connected to the output of the right leg drive amplifier (Fig. 9).

Figure 10 shows a sample electrocardiogram recorded in a Faraday cage using the single ended 2-electrode configuration. The raw signal shows significant power-line interference, and it is quite difficult to make out any features in the electrocardiogram. After adaptive filtering [39], the QRS spike is observable.

Figure 11 shows a sample electrocardiogram recorded using the "pseudo 2-electrode" configuration. The two electrodes (in one of which the outer ring was the driven electrode) were pressed across the heart. Power-line interference is not noticeable, and the adaptive filter is unnecessary.

VI. Practical tips

Based on our experience in designing an electrocardiograph, we offer the following gotchas.

[1]The complete schematic and software are available under an open source license at https://github.com/s-gv/ecg

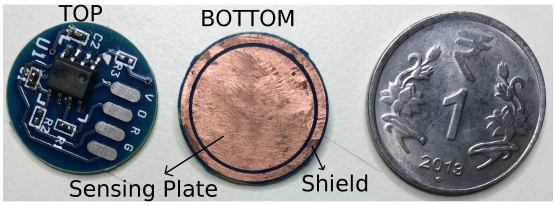

(a) Electrodes (Diameter $\approx$ 18 mm)

Fig. 9. Photo of the wearable electrocardiograph. Two such circular physical electrodes are used. In one of the electrodes, the outer ring (shield) on the back copper side is connected to the right-leg-drive amplifier. In the second electrode, the outer ring is left floating.

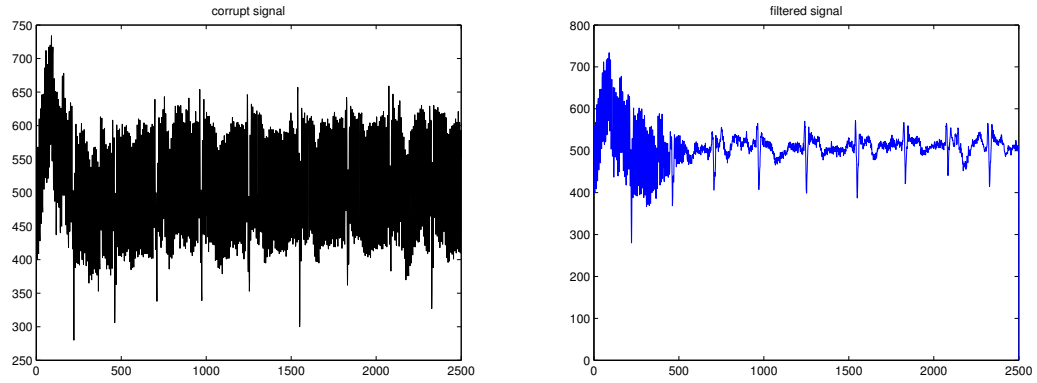

(a) Raw electrocardiogram

(b) Filtered electrocardiogram

Fig. 10. A sample electrocardiogram recorded using two electrodes in the single ended mode

- ***Waveforms in the oscilloscope are better than they appear***. In some bench-top oscilloscopes, one of the terminals of the probe is connected to earth ground. So, connecting such a probe to the ECG interface circuit effectively makes $Z_s = 0$. Even otherwise, bench-top oscilloscopes are usually mains powered, which substantially decreases the isolation impedance (from 0.1-1 pF to 10 pF). Consequently, if you are observing voltages on a battery powered ECG interface circuit using a line-powered oscilloscope, expect to see 10-100x more power-line interference than if you don't connect the oscilloscope.
- ***Battery charger corrupts ECG signals***. When prototyping electrocardiographs, be vary of the power source. It's not that you need a very clean power source devoid of 50 Hz interference. The real problem is how much isolation impedance there is between the power source and the earth ground. If you're designing battery powered equipment, do *not* use mains powered bench-top power supplies or draw power from a USB cable attached to a mains powered PC when prototyping. The power-line interference will be 10-100x higher than if you used a battery powered circuit because of the lowered isolation impedance. It is acceptable to draw power from the USB port of a laptop when prototyping. But do not forget to remove the battery charger from the laptop! Also, if you're using a laptop as the power source, keep the laptop and the interface circuit PCB on your lap rather than on a table nearby.
- ***Large power-line noise despite using a 50 Hz notch filter***. Notch filters are unforgiving to frequency deviations. If you have a steep notch filter that rejects 50 Hz interference, it'll do a fairly bad job if the power line frequency is 49 Hz and not 50 Hz. The situation can be worse if an analog notch filter is used (because of component tolerances). Furthermore, notch filters tend to cause ringing artifacts near the QRS spike. An adaptive filter [39] is immune to these problems and should thus be preferred[2].
- ***Underestimating the electrode-skin impedance***. The electrode-skin impedance for dry/non contact electrodes is quite high. So, the amplifier has to be placed very close to the skin to ensure that input impedance is large. Otherwise, the parasitic impedance of the wire will form a potential divider with the electrode impedance and cause substantial attenuation of the ECG signal (Fig. 12).

VII. Open Issues

Dry-contact electrodes were demonstrated decades ago [18]. Despite the convenience they offer, dry-contact electrodes have not seen widespread deployment. One of the reasons is that they are much more susceptible to motion artifacts than gel-based wet electrodes. In wet electrodes, the gel, in addition to lowering the electrode impedance, also serves as an adhesive and

[2]An open source implementation of the adaptive filter in [39] is available at https://github.com/s-gv/ecg/blob/master/adaptive_filter/pll_martens_errorfilt_supp.m

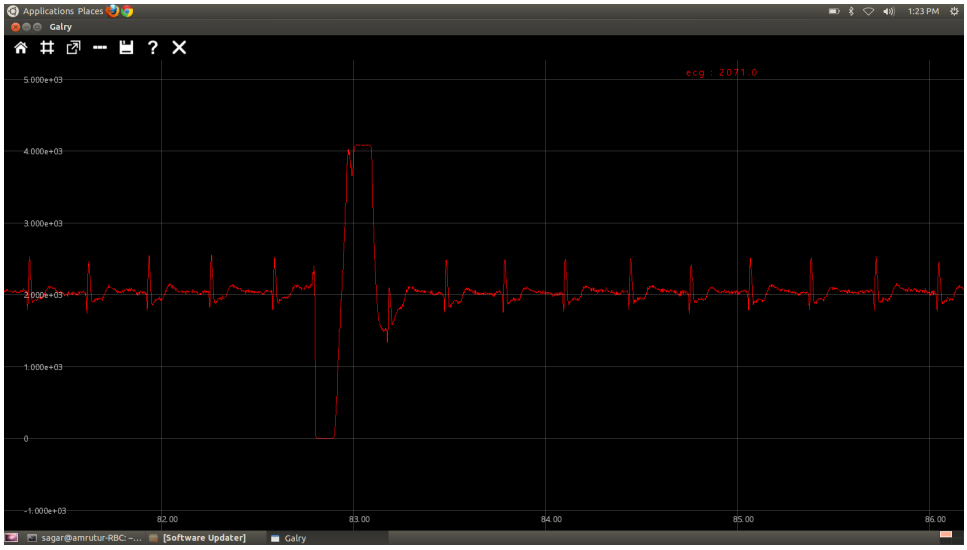

Fig. 11. A sample electrocardiogram recorded using "pseudo 2-electrodes"

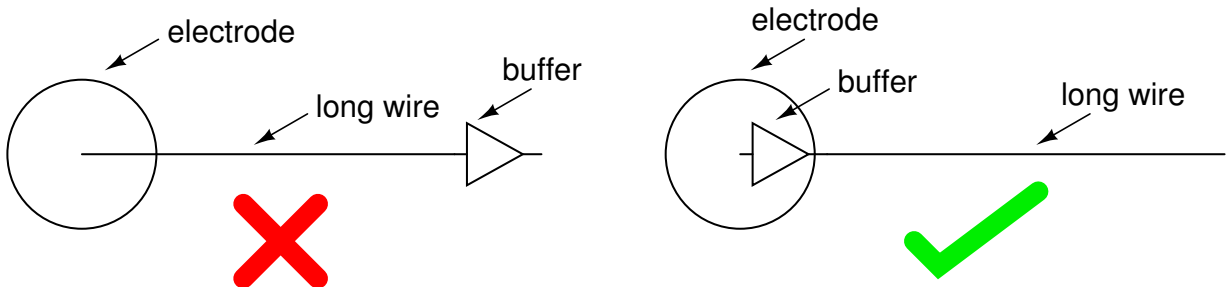

Fig. 12. How to not build an electrode with a long cable

reduces the relative motion between the skin and the electrode, thereby reducing motion artifacts. In dry electrodes, however, there is nothing to prevent relative motion between the electrodes and the skin. The prevailing opinion is that a mechanical (product design) solution is needed to solve this problem [26]. It remains open if the problem of motion artifacts can be solved by clever artifact cancelling algorithms.

Another open issue with dry-contact electrodes is the size of the electrodes. To the best of our knowledge, no systematic study that recommends a particular size for the high-impedance and low-impedance electrodes has been done, and there has been no discussion on whether PCB layout or product design strategies can help reduce the electrode size.

Currently, even in wireless ECG systems, the electrodes need to be connected by wires. At the time of writing, no truly wireless ECG system exists. In such a system, the electrodes will have a wireless module and can work without any wires. The question of how build such a fully wireless electrocardiograph (with wireless electrodes) remains open.

Finally, existing electrocardiograph designs in the literature do not attempt minimize the number of off-chip components when using a popular commercially available SoCs that include a radio and a microcontroller (example: TI's CC2540). It is desirable to reduce the number of analog components required to build an electrocardiograph because it will help in making a compact product without resorting to expensive custom integrated circuits. Multiple amplifiers are currently needed to build an electrocardiograph. It would be worthwhile exploring if an electrocardiograph can be built with few off-chip components by exploiting peripherals available in a microcontroller platform.

VIII. Conclusion

An electrical model of the human body was presented. This model explained the superior performance of the right-leg-driven interface circuit from the perspective of power-line interference. An adaptive filter was found to be most suitable in removing any remnant power-line interference in two-electrode systems. Our analysis showed that in three electrode systems, the driven electrode can be sized smaller than the sensing electrodes while still reaping the benefits of lower power-line interference. A number of practical suggestions to aid prototyping battery powered ECG systems were given, and some open issues were discussed.

ACKNOWLEDGMENT

The authors thank the Robert Bosch Center for Cyber-Physical Systems for funding support. We would also like to thank Pushkar and Manikandan for fruitful discussions, and Dhruv Saxena for product design assistance.

REFERENCES

[1] C. D. Mathers, R. Sadana, J. A. Salomon, C. J. Murray, and A. D. Lopez, "Healthy life expectancy in 191 countries," *The Lancet*, vol. 357, no. 9269, pp. 1685–1691, 2001.
[2] J. A. Salomon, H. Wang, M. K. Freeman, T. Vos, A. D. Flaxman, A. D. Lopez, and C. J. Murray, "Healthy life expectancy for 187 countries, 1990–2010: A systematic analysis for the global burden disease study," *The Lancet*, vol. 380, no. 9859, pp. 2144–2162, 2013.
[3] J. Lubitz, L. Cai, E. Kramarow, and H. Lentzner, "Health, life expectancy, and health care spending among the elderly," *New England Journal of Medicine*, vol. 349, no. 11, pp. 1048–1055, 2003.
[4] P. A. Heidenreich, J. G. Trogdon, O. A. Khavjou, J. Butler, K. Dracup, M. D. Ezekowitz, E. A. Finkelstein, Y. Hong, S. C. Johnston, A. Khera *et al.*, "Forecasting the future of cardiovascular disease in the united states: A policy statement from the american heart association," *Circulation*, vol. 123, no. 8, pp. 933–944, 2011.
[5] D. Lloyd-Jones, R. J. Adams, T. M. Brown, M. Carnethon, S. Dai, G. De Simone, T. B. Ferguson, E. Ford, K. Furie, C. Gillespie *et al.*, "Heart disease and stroke statistics update: A report from the american heart association," *Circulation*, vol. 121, no. 7, pp. e46–e215, 2010.
[6] S. Stern and D. Tzivoni, "Early detection of silent ischaemic heart disease by 24-hour electrocardiographic monitoring of active subjects." *British heart journal*, vol. 36, no. 5, p. 481, 1974.
[7] H. Rao, D. Saxena, S. Kumar, S. V. Gubbi, B. Amrutur, P. Mony, P. Thankachan, K. Shankar, S. Rao, and S. R. Bhat, "Low power remote neonatal temperature monitoring device," in *7th International Conference on Biomedical Electronics and Systems, BIODEVICES*, 2014.
[8] C. R. Merritt, H. T. Nagle, and E. Grant, "Fabric-based active electrode design and fabrication for health monitoring clothing," *IEEE Transactions on Information Technology in Biomedicine*, vol. 13, no. 2, pp. 274–280, 2009.
[9] M. Steffen, A. Aleksandrowicz, and S. Leonhardt, "Mobile noncontact monitoring of heart and lung activity," *IEEE Transactions on Biomedical Circuits and Systems*, vol. 1, no. 4, pp. 250–257, 2007.
[10] J. Yoo, L. Yan, S. Lee, H. Kim, and H.-J. Yoo, "A wearable ECG acquisition system with compact planar-fashionable circuit board-based shirt," *IEEE Transactions on Information Technology in Biomedicine*, vol. 13, no. 6, pp. 897–902, 2009.
[11] T.-H. Kang, C. R. Merritt, E. Grant, B. Pourdeyhimi, and H. T. Nagle, "Nonwoven fabric active electrodes for biopotential measurement during normal daily activity," *IEEE Transactions on Biomedical Engineering*, vol. 55, no. 1, pp. 188–195, 2008.
[12] L. Fay, V. Misra, and R. Sarpeshkar, "A micropower electrocardiogram amplifier," *IEEE Transactions on Biomedical Circuits and Systems*, vol. 3, no. 5, pp. 312–320, 2009.
[13] O. T. Inan and G. T. Kovacs, "An $11mu$ w, two-electrode transimpedance biosignal amplifier with active current feedback stabilization," *IEEE Transactions on Biomedical Circuits and Systems*, vol. 4, no. 2, pp. 93–100, 2010.
[14] T. Dawber, W. Kannel, D. Love, and R. Streeper, "The electrocardiogram in heart disease detection: A comparison of the multiple and single lead procedures," *Circulation*, vol. 5, no. 4, pp. 559–566, 1952.
[15] N. V. Thakor and J. G. Webster, "Ground-free ECG recording with two electrodes," *IEEE Transactions on Biomedical Engineering*, no. 12, pp. 699–704, 1980.
[16] I.-D. Hwang and J. G. Webster, "Direct interference canceling for two-electrode biopotential amplifier," *IEEE Transactions on Biomedical Engineering*, vol. 55, no. 11, pp. 2620–2627, 2008.
[17] J. J. Bailey, A. S. Berson, A. Garson Jr, L. G. Horan, P. W. Macfarlane, D. W. Mortara, and C. Zywietz, "Recommendations for standardization and specifications in automated electrocardiography: bandwidth and digital signal processing. a report for health professionals by an ad-hoc writing group of the committee on electrocardiography and cardiac electrophysiology of the council on clinical cardiology, american heart association." *Circulation*, vol. 81, no. 2, p. 730, 1990.
[18] A. Lopez and P. C. Richardson, "Capacitive electrocardiographic and bioelectric electrodes," *IEEE Transactions on Biomedical Engineering*, no. 1, pp. 99–99, 1969.
[19] M. Ishijima, "Monitoring of electrocardiograms in bed without utilizing body surface electrodes," *IEEE Transactions on Biomedical Engineering*, vol. 40, no. 6, pp. 593–594, 1993.
[20] T. J. Sullivan, S. R. Deiss, and G. Cauwenberghs, "A low-noise, non-contact EEG/ECG sensor," in *IEEE Biomedical Circuits and Systems Conference*, 2007, pp. 154–157.
[21] Y. M. Chi, S. R. Deiss, and G. Cauwenberghs, "Non-contact low power EEG/ECG electrode for high density wearable biopotential sensor networks," in *IEEE Sixth International Workshop on Wearable and Implantable Body Sensor Networks*, 2009, pp. 246–250.
[22] Y. M. Chi, P. Ng, E. Kang, J. Kang, J. Fang, and G. Cauwenberghs, "Wireless non-contact cardiac and neural monitoring," in *Wireless Health*. ACM, 2010, pp. 15–23.
[23] Y. M. Chi and G. Cauwenberghs, "Wireless non-contact EEG/ECG electrodes for body sensor networks," in *IEEE International Conference on Body Sensor Networks (BSN)*, 2010, pp. 297–301.
[24] ——, "Micropower non-contact eeg electrode with active common-mode noise suppression and input capacitance cancellation," in *Annual International Conference of the IEEE Engineering in Medicine and Biology Society*, 2009, pp. 4218–4221.
[25] T. J. Sullivan, S. R. Deiss, T.-P. Jung, and G. Cauwenberghs, "A brain-machine interface using dry-contact, low-noise EEG sensors," in *IEEE International Symposium on Circuits and Systems*, 2008, pp. 1986–1989.
[26] Y. Chi, T.-P. Jung, and G. Cauwenberghs, "Dry-contact and noncontact biopotential electrodes: Methodological review," *IEEE Reviews in Biomedical Engineering*, vol. 3, pp. 106–119, 2010.
[27] W. P. Holsinger and K. M. Kempner, "Portable ekg telephone transmitter," *IEEE Transactions on Biomedical Engineering*, no. 4, pp. 321–323, 1972.
[28] D. Dobrev and I. Daskalov, "Two-electrode biopotential amplifier with current-driven inputs," *Medical and Biological Engineering and Computing*, vol. 40, no. 1, pp. 122–127, 2002.
[29] D. Dobrev, "Two-electrode low supply voltage electrocardiogram signal amplifier," *Medical and Biological Engineering and Computing*, vol. 42, no. 2, pp. 272–276, 2004.
[30] D. P. Dobrev, T. Neycheva, and N. Mudrov, "Bootstrapped two-electrode biosignal amplifier," *Medical & biological engineering & computing*, vol. 46, no. 6, pp. 613–619, 2008.
[31] E. M. Spinelli and M. A. Mayosky, "Two-electrode biopotential measurements: power line interference analysis," *IEEE Transactions on Biomedical Engineering*, vol. 52, no. 8, pp. 1436–1442, 2005.
[32] B. B. Winter and J. G. Webster, "Reductionl of interference due to common mode voltage in biopotential amplifiers," *IEEE Transactions on Biomedical Engineering*, no. 1, pp. 58–62, 1983.
[33] J. C. Huhta and J. G. Webster, "60-hz interference in electrocardiography," *IEEE Transactions on Biomedical Engineering*, no. 2, pp. 91–101, 1973.
[34] B. B. Winter and J. G. Webster, "Driven-right-leg circuit design," *IEEE Transactions on Biomedical Engineering*, no. 1, pp. 62–66, 1983.

[35] T. Degen and H. Jackel, "Enhancing interference rejection of preamplified electrodes by automated gain adaption," *IEEE Transactions on Biomedical Engineering*, vol. 51, no. 11, pp. 2031–2039, 2004.
[36] B. Widrow, J. R. Glover Jr, J. M. McCool, J. Kaunitz, C. S. Williams, R. H. Hearn, J. R. Zeidler, E. Dong Jr, and R. C. Goodlin, "Adaptive noise cancelling: Principles and applications," *Proceedings of the IEEE*, vol. 63, no. 12, pp. 1692–1716, 1975.
[37] N. V. Thakor and Y.-S. Zhu, "Applications of adaptive filtering to ecg analysis: noise cancellation and arrhythmia detection," *IEEE Transactions on Biomedical Engineering*, vol. 38, no. 8, pp. 785–794, 1991.
[38] A. K. Ziarani and A. Konrad, "A nonlinear adaptive method of elimination of power line interference in ecg signals," *IEEE Transactions on Biomedical Engineering*, vol. 49, no. 6, pp. 540–547, 2002.
[39] S. M. Martens, M. Mischi, S. G. Oei, and J. W. Bergmans, "An improved adaptive power line interference canceller for electrocardiography," *IEEE Transactions on Biomedical Engineering*, vol. 53, no. 11, pp. 2220–2231, 2006.
[40] S. Nishimura, Y. Tomita, and T. Horiuchi, "Clinical application of an active electrode using an operational amplifier," *IEEE Transactions on Biomedical Engineering*, vol. 39, no. 10, pp. 1096–1099, 1992.
[41] T. Degen and H. Jackel, "A pseudodifferential amplifier for bioelectric events with dc-offset compensation using two-wired amplifying electrodes," *IEEE Transactions on Biomedical Engineering*, vol. 53, no. 2, pp. 300–310, 2006.
[42] R. Pallas-Areny, J. Colominas, and J. Rosell, "An improved buffer for bioelectric signals," *IEEE Transactions on Biomedical Engineering*, vol. 36, no. 4, pp. 490–493, 1989.